

## Effect of the dimethylsilyloxy co-monomer “D” on the chemistry of polysiloxane pyrolysis to SiOC



Martina Havelcová<sup>a,\*</sup>, Adam Strachota<sup>b</sup>, Martin Černý<sup>a</sup>, Zbyněk Sucharda<sup>a</sup>,  
Miroslav Šlouf<sup>b</sup>

<sup>a</sup> Institute of Rock Structure and Mechanics, Academy of Sciences of the Czech Republic, v.v.i., V Holesovickach 41, CZ-182 09 Praha, Czech Republic

<sup>b</sup> Institute of Macromolecular Chemistry, Academy of Sciences of the Czech Republic, v.v.i., Heyrovského Namesti 2, CZ-16200 Praha, Czech Republic

### ARTICLE INFO

#### Article history:

Received 26 January 2015

Received in revised form

10 December 2015

Accepted 22 December 2015

Available online 29 December 2015

#### Keywords:

Silicon oxycarbide

Siloxane

Pyrolysis

### ABSTRACT

The effect of the dimethylsilyloxy co-monomer “D” on the chemistry of polysiloxane pyrolysis to silicon oxycarbide (SiOC) glass was studied with the aim of its optimization for the preparation of refractory composites with ceramic fibers. Reasonably small weight losses (shrinkage), but also some temporary plasticity of the material during its pyrolysis was sought. The pyrolysis chemistry was varied by preparing precursors from methyltriethoxysilane (T; main monomer) and dimethyldiethoxysilane (D; co-monomer) in different ratios, but also by using an alternative composition based on tetraethoxysilane (Q) and D. Pyrolysis temperatures between 300 and 1000 °C were studied, and the escaping gases – polar, as well as non-polar – were analysed by means of chromatography/mass spectrometry. It was demonstrated, that the co-monomer D, which undergoes thermal elimination and subsequent reactions with the siloxane skeleton, seems to be responsible for the generally useful “micro-creep” ability of the pyrolyzing material. At higher D contents, where the pyrolysis weight losses strongly increase, the pyrolysis gases were shown to contain also polycyclic oligomers, which consist not only of D, but of the branching T or Q “main” monomers as well. The Si–O/Si–C exchange reactions of escaping D with the skeleton were found to be highly efficient not only in T/D, but also in Q/D polysiloxanes. It was further found, that the SiOC products after completed pyrolysis at 1000 °C still can release gases detectable by GC/MS upon repeated heating, although no significant weight losses are observed: this indicates the presence of small amounts of pyrolysable sediments in micro- and nano-pores of the SiOC glass.

© 2015 Elsevier B.V. All rights reserved.

### 1. Introduction

Silicon oxycarbide glass (SiOC) is a material of considerable interest due to its good oxidation resistance and to its structural stability at elevated temperatures [1–3]. The most popular route to SiOC is the pyrolysis of siloxane precursor polymers under an inert atmosphere, at temperatures between 800 and 1200 °C. The so-obtained product is not entirely homogeneous but contains nano-domains of SiO<sub>2</sub>, Si<sub>x</sub>O<sub>y</sub>C<sub>z</sub>, as well as C-rich domains [2,4], which can further differentiate and grow in size at temperatures above 1200 °C [4]. The pyrolysis process is accompanied by considerable shrinkage, which even can exceed 40 vol.% [5], and by the evolution of considerable amounts of pyrolysis gases. In case of larger three-dimensional samples, differences in the progress

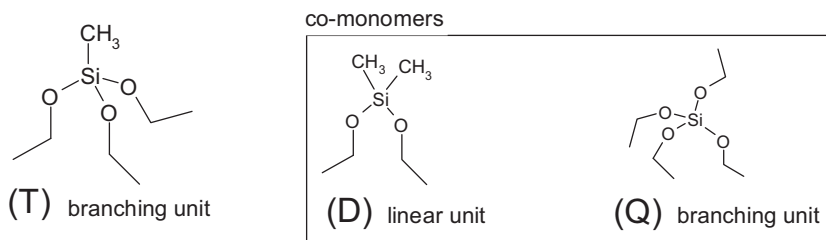
of shrinkage, as well as temperature gradients, generate residual stresses resulting in cracking and brittleness of the sample.

One successful path to large monolithic SiOC specimens is the preparation of products with open-cell porosity, micro- [6] or multi-scale [7–11] which enables a smooth escape of pyrolysis gases. The build-up of residual stresses in the solid is strongly reduced due to relatively thin pore walls.

Another possibility of obtaining large three-dimensional specimens of SiOC-based material is the preparation of composites of SiOC matrix with refractory fillers, e.g., ceramic or carbon fibres. SiOC fibres produced according to [12] could be employed to produce compact SiOC/SiOC composites. SiOC composites with ceramic or carbon fibres were explored in some previous works of the authors [13–15]. These products typically displayed a macro-porosity of 5–10%, their pores were oriented and did not negatively affect the high mechanical properties (strength, Young- and shear modulus, creep resistance) of the final material. An interesting product group are SiOC/basalt fibre composites, whose

\* Corresponding author.

E-mail address: [havelcova@irms.cas.cz](mailto:havelcova@irms.cas.cz) (M. Havelcová).



**Scheme 1.** The main monomer T, the alternative main monomer Q, and the co-monomer D used in this work.

preparation requires relatively low final pyrolysis temperatures of only 600–750 °C (partly pyrolyzed composites) [5,14,15], due to the limited thermal stability of basalt. The so-prepared composites display very good fracture toughness and a distinct fibre pull-out effect [14,15], in contrast to SiOC/ceramic fibre composites prepared in [13]. This difference is due to relatively strong interface bonding between SiOC and ceramic fibres on one hand, and relatively weak bonding between SiOC and basalt on the other.

In the recent years, most of the works dedicated to SiOC focus on designing paths to products with a hierarchical pore structure [6–11]. Concerning the chemistry of polysiloxanes pyrolysis (of simple as well as of hydrido-modified ones), the most important findings were reported by Campostrini et al. [16], who also discussed Si–O/Si–C exchange reactions during the process. The latter reactions were also discussed by Mutin [17] and play a key role in the formation of the final glassy structure of SiOC.

The aim of this work was a detailed study of the role of the linear dimethylsilyloxy co-monomer (D) in the temporary “micro-creep” behavior of some polysiloxanes during their pyrolysis to SiOC, and the clarification of the chemical mechanism of this “micro-creep”, in the context of the potential application of the so-obtained SiOC as matrix in refractory composites with ceramic fibres. Reasonably small shrinkage (weight losses), and also some temporary plasticity of the material during pyrolysis were sought. The efficiency of Si–O/Si–C exchange reactions in polysiloxanes of the T/D type and in the alternative Q/D resins was to be compared (main monomers: T = methyltriethoxysilane, Q = tetraethoxysilane). Q/D resins should pyrolyze to quartz glass and gaseous D oligomers if no exchange reactions occur. Besides the escaping siloxane oligomers, also non-polar pyrolysis gases (hydrocarbons, silanes) were to be analysed thoroughly. The stability of the final SiOC product, namely its ability to release gases upon repeated heating, was also to be tested.

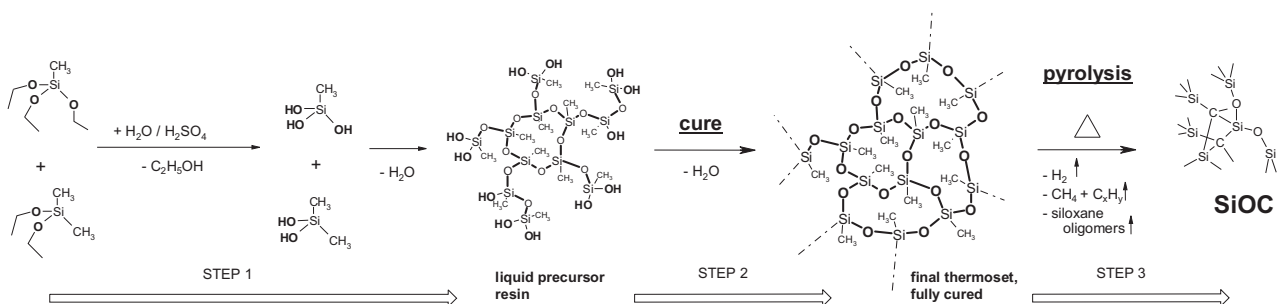
In their previous work [18,19], the authors studied the optimization of sol-gel/pyrolysis routes to silicon oxycarbide glasses, while employing methyltriethoxysilane T, D and Q as starting compounds, as well as several derivatives of T and D. It was found that simple T/D polysiloxanes resins start to display excessive pyrolysis

weight losses at the D: T ratio of 1 or higher, while at T: D ratios over 4, the resins' gelation upon cure becomes too fast. In case of the alternative Q/D compositions also studied in [19], the resin Q1D3 is equivalent to T1D1 (not T1D3), if the theoretical crosslinking density is considered. Q1D3 was found to display the most promising properties among the Q/D resins: at lower D contents, an increasingly abrupt gelation upon cure is observed, while at higher D contents, the pyrolysis weight losses (which are already considerable in Q1D3) become excessive. Hence the compositions T2D1, T3D1 and T4D1, as well as Q1D3 appeared to be most promising for the eventual application as precursors of refractory composite matrices, and were chosen for the detailed pyrolysis study done in this work.

## 2. Experimental part

### 2.1. Preparation of precursor resins and of silicon oxycarbide glass

The detailed preparation procedure of SiOC (sol-gel/pyrolysis) which was used by the authors in this work has been reported in their previous papers [18,19]. The procedure consists of three steps (see Scheme 2): first, a storable toluene solution of a liquid, low-molecular-weight polysiloxane was prepared via acid catalysed (4 wt.% H<sub>2</sub>SO<sub>4</sub>) hydrolysis followed by condensation (sol-gel process) of selected mixtures of the alkoxy-silanes shown in Scheme 1. In this way, the resins Q<sub>1</sub>D<sub>3</sub>, T<sub>2</sub>D<sub>1</sub>, T<sub>3</sub>D<sub>1</sub>, and T<sub>4</sub>D<sub>1</sub> were obtained, in which the coefficients indicate the ratios of the starting monomers. A sample with the stoichiometry T<sub>1</sub>D<sub>1</sub> and another one based exclusively on the T monomer were also prepared and used for some comparative tests. In the second preparation step, the solvent was removed from the liquid precursor resin at 50 °C under vacuum, and the resin was subsequently cured under air at the temperature rising up to 250 °C (see T-program in Fig. 1), thus yielding an infinite polysiloxane network (solid precursor). In the third and final step, the solid precursor was pyrolyzed in nitrogen at the temperature rising up to 1000 °C (T-program: Fig. 1), thus yielding the purely inorganic SiOC. Selected samples were pyrolyzed to lower final



**Scheme 2.** The process of SiOC preparation: Synthesis of low-molecular-weight resin solution (liquid precursor) via hydrolysis/condensation (sol-gel process) of alkylalkoxy-silanes, shown on the example of the monomers T and D (step 1); subsequent cure of the liquid precursor (step 2) yields an infinite siloxane polymer network (solid precursor); the solid precursor is finally pyrolyzed to SiOC (step 3).

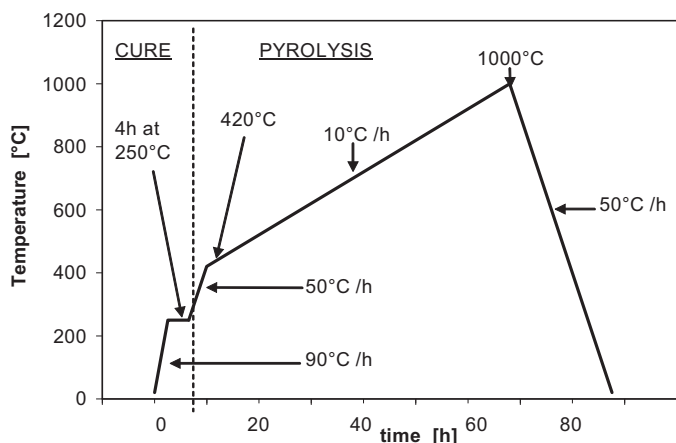


**Fig. 1.** Temperature program of: resin cure (far left) and of pyrolysis of the cured precursor (right): full pyrolysis was performed up to 1000 °C. Partly pyrolyzed samples were also prepared in an analogous way, reaching maximum temperatures of 300, 400, 500, 650 and 750 °C instead of 1000 °C.

temperatures (300, 400, 500, 650 and 750 °C), using an analogous T-program like in Fig. 1.

## 2.2. Thermogravimetry and weight loss analysis

Thermogravimetry (TGA) experiments were carried out on a Setsys Evolution 1750 instrument from Setaram Instrumentation (Caluire, France).

- In order to assess the content of D oligomers and of other volatile compounds, the time dependence of the weight of the cured, non-pyrolyzed resins was measured at the constant temperature of 200 °C, in air.
- Characteristic temperature regions of the pyrolysis process were assessed by recording TGA traces of cured resin samples, which were heated in a helium atmosphere up to 900 °C, at the rate of 10 °C/min. Additionally, a “slow” TGA experiment was conducted with a cured T<sub>2</sub>D<sub>1</sub> sample: it was heated under nitrogen following a temperature program identical with the one (see Fig. 1) used for pyrolysis of standard samples up to 1000 °C.
- Weight losses of the studied samples after completion of the cure and of the pyrolysis up to different final temperatures were determined by weighing the samples before and after the respective treatment.

## 2.3. Pyrolysis-GC/MS analysis

Pyrolysis coupled with gas chromatography and product identification via mass spectroscopy (Py-GC/MS) was performed using a CDS Pyroprobe 5150 chamber connected to a Trace Ultra GC, which in turn was connected to a quadrupole MS spectrometer Thermo DSQ II.

Powdered 2 mg samples of cured, partly, or fully pyrolyzed resins were put into the heated sampling chamber and subjected for 30 s to a given constant temperature: cured samples were heated at 160 and at 200 °C in order to detect the escape of volatile siloxane oligomers. The pyrolyzed samples were heated at the final temperature, which they had previously achieved, namely at 300, 400, 500, 650, 750, and 1000 °C, respectively, in order to obtain pyrolysis gases characteristic of the respective temperature. The so obtained pyrolysis gases were conducted through an interface into a GC column. The interface was kept at the maximum allowed temperature of 300 °C, while the temperature of the GC column was programmed to increase from 35 to 300 °C at 5 °C min<sup>-1</sup>. Helium

was used as carrier gas. Two different columns were employed, in order to analyse either the polar, or the non-polar pyrolysis products: TR-5MS (25 m × 0.25 mm internal diameter), and Restec Rt-Alumina (30 m × 0.32 mm internal diameter), respectively. Mass spectra of the isolated substances were recorded in the electron impact mode (70 eV), in the *m/z* range of 40–500. Compound identification was done by comparing the obtained MS spectra with the ones included in the NIST library, or with literature data [20].

## 2.4. Scanning electron microscopy (SEM) and EDX elemental analysis

The morphology of the prepared SiOC ceramics was studied by scanning electron microscopy (SEM) using the Quanta 200 FEG microscope from FEI. Freshly broken surfaces were used for the analyses. Micrographs were obtained with a secondary electron detector at an accelerating voltage of 10 kV. Elemental analyses were performed using an EDS detector (EDX). The EDX spectra was taken at 30 kV and the signal was collected from sample areas of 250 × 500 μm.

## 3. Results

### 3.1. Temperature-dependent weight loss behavior

#### 3.1.1. Volatile siloxane oligomers in the cured resins

Fig. 2 shows the time-dependent weight losses of the cured resins Q<sub>1</sub>D<sub>3</sub>, T<sub>2</sub>D<sub>1</sub>, T<sub>3</sub>D<sub>1</sub> and T<sub>4</sub>D<sub>1</sub> at the constant temperature of 200 °C in air, 50 °C below the cure temperature. Weight losses below 1% (T/D resins) or below 2% (Q<sub>1</sub>D<sub>3</sub> resin) were observed after 280 h. After 130 h, the weight loss slows down considerably, but continues at a small rate even after 280 h. The weight losses observed at 200 °C increase with the amount of the D monomer in the cured resins. The effect can be assigned to the evaporation of cyclic D oligomers (boiling points of D-cyclo-trimer and D-cyclo-tetramer are well below 200 °C), which were formed from the monomer D as by-products of the sol-gel process (resin synthesis) shown in Scheme 2.

#### 3.1.2. TGA trace of the pyrolysis process: characteristic weight loss temperatures

The mass losses during the transformation of cured polysiloxanes (Q<sub>1</sub>D<sub>3</sub>, T<sub>2</sub>D<sub>1</sub>, T<sub>3</sub>D<sub>1</sub>, T<sub>4</sub>D<sub>1</sub>) into SiOC glasses were followed by means of thermogravimetry (TGA: see Fig. 3 with different zoom in each graph). As will be discussed below, a large part of the D monomer is observed to eliminate from the tested precursors.

The temperatures of decomposition onset and of the maximal decomposition rate (see Fig. 3) strongly depend on the content of the co-monomer D: the precursors with the highest D content, Q<sub>1</sub>D<sub>3</sub> and T<sub>2</sub>D<sub>1</sub>, display the lowest decomposition onset temperatures (*T* of 1% wt. loss), 320 °C and 350 °C, respectively. With decreasing D content, the onset temperature rises up to 500 °C in the case of T<sub>4</sub>D<sub>1</sub>.

The first major decomposition (and the main one in most samples) occurs near 500 and 600 °C, where two adjacent broad dTG peaks are observed in resins rich in D (Fig. 3). The resins which are the richest in D, namely Q<sub>1</sub>D<sub>3</sub> and T<sub>2</sub>D<sub>1</sub>, additionally display distinct sharp and intense dTG peaks (stemming from TGA curve steps) at 525 °C and 585 °C, respectively, which are situated on top of the mentioned broader peaks. The intensity of these sharp peaks decreases with decreasing D content (they are absent in T<sub>3</sub>D<sub>1</sub> and T<sub>4</sub>D<sub>1</sub>). Also the underlying broader peaks lose prominence with decreasing D content: the 500 °C peak is no more distinct in T<sub>3</sub>D<sub>1</sub> and T<sub>4</sub>D<sub>1</sub>; moreover, in T<sub>4</sub>D<sub>1</sub>, the 600 °C peak is less intense than the next following decomposition peak at 730 °C. The observed results suggest the assignment of the decomposition peaks near

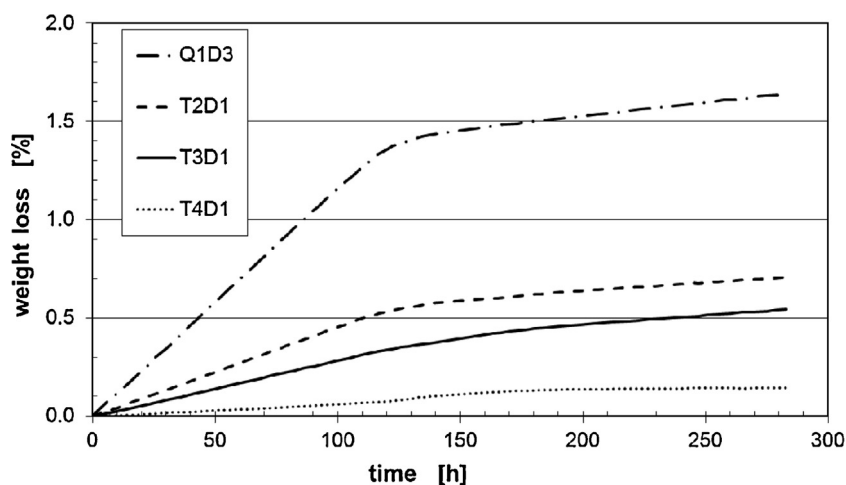


Fig. 2. Time-dependent weight loss of the cured polysiloxane resins at the constant temperature of 200 °C.

500 and 600 °C to the thermal elimination of D units from different bonding situations in the polysiloxane polymer. The spike-like additional peaks indicate a simple process, like the depolymerization of different short D sequences (in  $Q_1D_3$  two such peaks are observed).

A second major decomposition observed in all samples (its intensity is weak in  $Q_1D_3$ ) is indicated by a broad dTG peak near 730 °C. This peak is probably the result of Si–C bonds cracking and of Si–O/Si–C exchange processes, which lead to the release of hydrocarbons and hydrogen. In the dTG spectrum of  $T_4D_1$ , the peak at 730 °C is the most prominent one, as only few D units can be lost by elimination. Additionally, as will be discussed further

below, the process of elimination of polycyclic oligomers (including silsesquioxane cages) seems to extend over both the first and the second decomposition regions, although it is more prominent (and probably facilitated by exchange reactions) in the second one.

The above discussed TGA analyses (Fig. 3) of precursor specimens were performed at a “fast” heating rate of 10 °C/min (whole TGA scan duration: ca. 1.67 h). On the other hand, the partly or fully pyrolyzed bulk samples, which were subjected to GC/MS analysis of escaping pyrolysis gases (see below), were prepared at a 60 times slower heating rate, namely at 10 °C/h (see exact pyrolysis program in Fig. 1; whole procedure duration: ca. 4 days). Such a slow pyrolysis rate during the preparation of bulk SiOC samples (e.g., as matrix

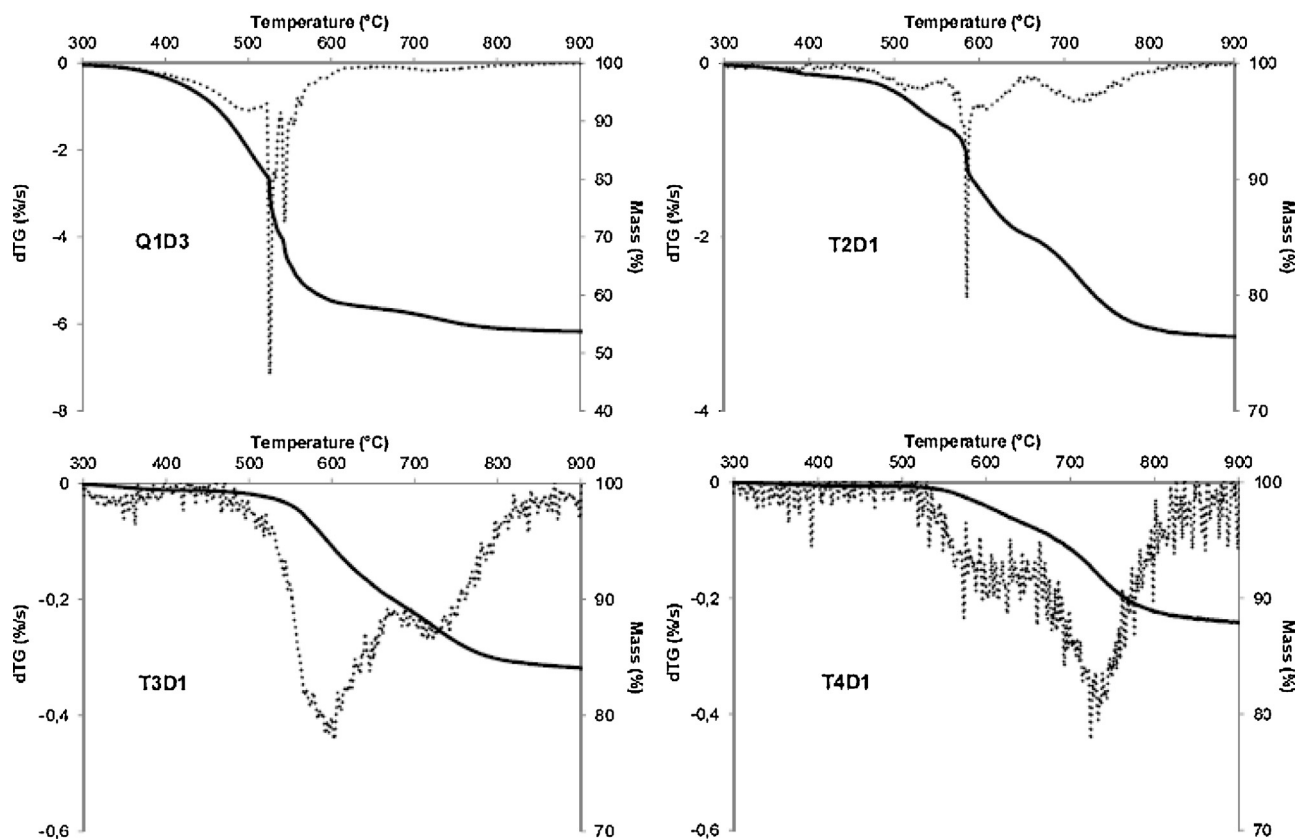
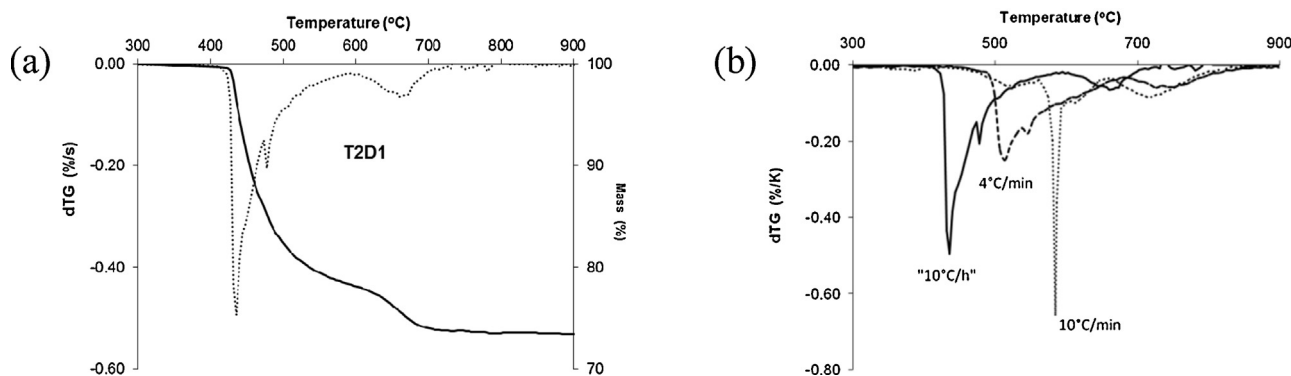


Fig. 3. TGA traces and differential thermograms (dTG) of the pyrolyses of the resins  $Q_1D_3$ ,  $T_2D_1$ ,  $T_3D_1$ ,  $T_4D_1$  to SiOC, measured at 10 °C/min, in helium atmosphere; the graphs are displayed at different zooms.



**Fig. 4.** (a): TGA trace and differential thermogram (dTG) of the cured resin T<sub>2</sub>D<sub>1</sub>, recorded under nitrogen and using the same T-program which was applied during sample cure and pyrolysis (see Fig. 1); (b) differential thermograms of T<sub>2</sub>D<sub>1</sub> pyrolyzed at different temperature rates: 10 °C/h, 4 °C/min and 10 °C/min.

in refractory composites) is routinely employed in order to prevent their cracking. For the slowly pyrolyzed bulk samples, the above discussed decompositions occur at somewhat lower temperatures, as illustrated in Fig. 4 on the example of T<sub>2</sub>D<sub>1</sub>: if the heating rate is changed from 10 °C/min to 4 °C/min and finally to 10 °C/h, the position of the main dTG peak (assigned to D elimination) shifts from 585 to 514 and finally to 435 °C. The position of the high-temperature dTG peak, which is assigned to Si–O/Si–C exchange reactions, shifts from 750 to 660 °C as the heating rate decreases (only a very small difference is observed between the heating rates 10 and 4 °C/min).

A broad and flat dTG peak with maximum around 350 °C, which is barely visible in T<sub>x</sub>D<sub>y</sub> samples (see Fig. 3), might be assigned to the evaporation of small amounts of volatile cyclic siloxane oligomers. The latter are present as a by-product in the cured resins prior to pyrolysis. In case of lower heating rates (as tested on T<sub>2</sub>D<sub>1</sub>), this flat and weak maximum (not visible with the zoom and axes' scales in Fig. 4) shifts to distinctly lower temperatures, from 350 (at 10 °C/min) to 300 and finally to 240 °C (10 °C/h), which well corresponds with the assignment.

### 3.1.3. Final weight losses after pyrolysis ending at different temperatures and the correlation between D monomer content and final weight loss at 1000 °C

Weight losses after the standard “slow” pyrolysis (*T*-increase rate: 10 °C/h) of cured samples, which was conducted up to the final pyrolysis temperatures of 400, 500, 750 and 1000 °C (*T*-program: Fig. 1) are compared in Fig. 5 and display similar trends like the TGA traces and dTG curves in Fig. 3: by far the highest and the earliest weight losses are displayed by the D-rich Q<sub>1</sub>D<sub>3</sub> resin, which already achieves most of its weight loss upon reaching 500 °C. The T<sub>3</sub>D<sub>1</sub> and T<sub>4</sub>D<sub>1</sub> resins display only small losses up to 500 °C, and their losses strongly increase (to still relatively small values) at 750 °C, approaching the final weight loss values at this temperature. The T<sub>2</sub>D<sub>1</sub> precursor displays higher weight losses than the other T<sub>x</sub>D<sub>y</sub> resins, and its loss after pyrolysis up to 500 °C is already considerable.

The correlation between the final pyrolysis weight loss at 1000 °C (in wt.%) and the content of the D co-monomer (in wt.%) in

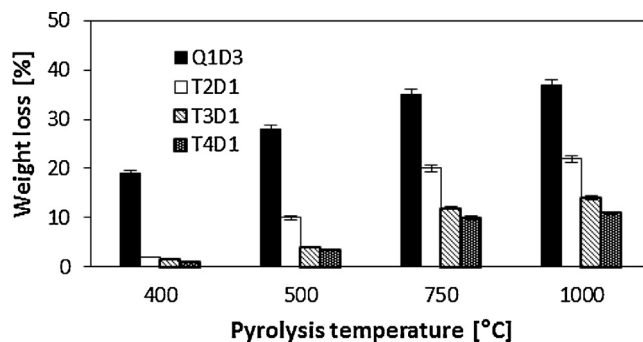


**Fig. 5.** Weight losses of cured polysiloxanes after pyrolysis in nitrogen at 400, 500, 750 and 1000 °C.

the precursor resin is shown in Fig. 6. A relatively good linearity is found ( $R^2 = 0.957$ ) and a simple fit indicates, that in the case of the investigated resins, the pyrolysis weight loss roughly corresponds to 50% of the weight of the incorporated D units.

A closer comparison, which takes into account also the losses of volatile siloxane oligomers during cure (see Table 1) indicates, that in the case of the T<sub>x</sub>D<sub>y</sub> resins with “very high” D contents (e.g., T<sub>1</sub>D<sub>1</sub> in Table 1), very large weight losses are achieved already during the cure. The high D content also most likely causes distinctly increased losses of the other monomer T (see GC/MS analyses further below). In contrast to this, the resin Q<sub>1</sub>D<sub>3</sub>, which has by far the highest weight content of the co-monomer D, displays the smallest pyrolysis weight loss relatively to the D content (47%) and also the distinctly smallest cure + pyrolysis weight loss relatively to the D content (61%, compared with 121% for T<sub>1</sub>D<sub>1</sub>, as shown in Table 1). This indicates a smaller degree of co-monomer D cyclization during the sol–gel synthesis of the Q<sub>1</sub>D<sub>3</sub> resin, as well as an efficient participation of D in Si–O/Si–C exchange reactions during the pyrolysis (see also chemistry discussion and Scheme 5 further below). The elemental composition of the final Q<sub>1</sub>D<sub>3</sub> pyrolysate – as determined by EDX – is influenced by the loss of carbon-rich D units during the pyrolysis (the branching main monomer Q is carbon-free), as well as by the participation of D in

**Table 1**  
Correlation between the content of D units and the pyrolysis weight losses or cure + pyrolysis weight losses in the studied polysiloxane resins.

Resin	wt.% of D units	Pyrolysis weight loss (%)	% of D corresponding to pyrolysis weight loss	Cure + pyrolysis weight loss (%)	% of D corresponding to cure + pyrolysis weight loss
T4D1	22	11 ± 1	50	19 ± 1	86
T3D1	27	14 ± 1	52	25 ± 1	93
T2D1	36	22 ± 1	62	38 ± 1	107
T1D1	53	28 ± 1	54	64 ± 1	121
Q1D3	79	37 ± 1	47	48 ± 1	61

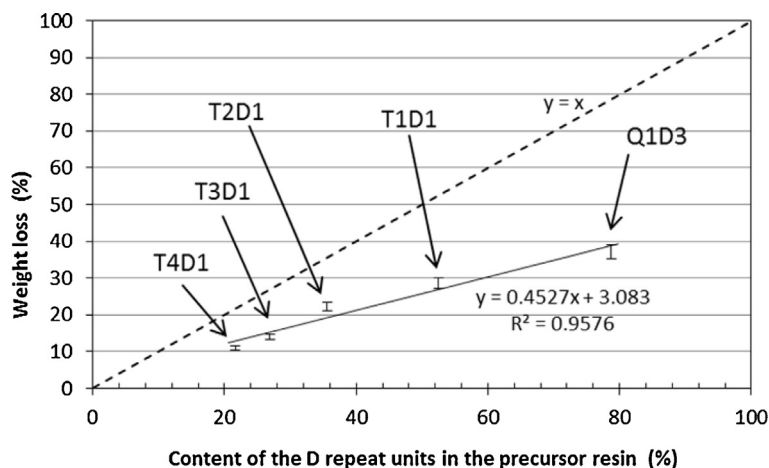


Fig. 6. Weight loss at 1000 °C (see TGA results shown in Fig. 5) on the content (wt.%) of the monomer D in particular resins.

Si–O/Si–C exchange reactions (which preserve some C originating from the D units). Hence, interestingly, all the SiOC glasses compared in this work display similar final stoichiometries, in spite of the different elemental ratios in the starting materials: T<sub>4</sub>D<sub>1</sub> and T<sub>3</sub>D<sub>1</sub>: SiO<sub>1.45 ± 0.05</sub>C<sub>0.2 ± 0.02</sub>; T<sub>2</sub>D<sub>1</sub> and Q<sub>1</sub>D<sub>3</sub> display a somewhat higher O and C content: SiO<sub>1.7 ± 0.05</sub>C<sub>0.5 ± 0.02</sub>.

### 3.2. GC/MS study of the pyrolysis chemistry

Exemplary GC/MS analyses of the pyrolysis gases escaping from the T<sub>1</sub>D<sub>4</sub> and Q<sub>1</sub>D<sub>3</sub> precursor resins are shown in Fig. 7a and b, respectively (assignment in Table 2 and Scheme 3, and in Fig. 8a and b). The analyses were performed with samples which were previously cured, and partly or fully pyrolyzed (*T*-program in Fig. 1)

until reaching the temperature of 300, 400, 500, 650, 750 or 1000 °C. Subsequently, pulverized specimens of these samples were heated again in the gas sampling chamber of the GC/MS apparatus, at the previously achieved highest pyrolysis temperature. The released gases, characteristic for that given temperature, were then analysed. Cured (non-pyrolyzed) resin samples were also subjected to GC/MS analysis of gases which they release at 160 and at 200 °C, in order to identify eventual volatile siloxane oligomers present in them.

The compounds escaping from the samples were analysed using two different chromatographic columns: (1) the TR-5MS column with a nonpolar silphenylene (5% Phenyl Polysilphenylene-siloxane) phase, which should be suitable for broad product spectra, but which poorly separates light hydrocarbons and similar unpolar

Table 2

Identified siloxane oligomers, their molecular weights, characteristic ions, and label codes used in the assigned gas chromatograms.

Label	Compound name	Formula	<i>M<sub>r</sub></i>	Characteristic ion
LS	Linear siloxanes			
LS1	Hexamethyldisiloxane	C <sub>6</sub> H <sub>18</sub> OSi <sub>2</sub>	162	147
LS2	Octamethyltrisiloxane	C <sub>8</sub> H <sub>24</sub> O <sub>2</sub> Si <sub>3</sub>	236	221
LS3	Decamethyltetrasiloxane	C <sub>10</sub> H <sub>30</sub> O <sub>3</sub> Si <sub>4</sub>	310	295
LS4	Phenylpentamethyldisiloxane	C <sub>11</sub> H <sub>20</sub> OSi <sub>2</sub>	224	209
CS	Cyclic siloxanes			
CS1	Hexamethylcyclotrisiloxane	C <sub>6</sub> H <sub>18</sub> O <sub>3</sub> Si <sub>3</sub>	222	207
CS2	Heptamethylcyclotetrasiloxane	C <sub>7</sub> H <sub>22</sub> O <sub>4</sub> Si <sub>4</sub>	282	267
CS3	Octamethylcyclotetrasiloxane	C <sub>8</sub> H <sub>24</sub> O <sub>4</sub> Si <sub>4</sub>	296	281
CS4	Octamethylcyclopentasiloxane	C <sub>8</sub> H <sub>26</sub> O <sub>5</sub> Si <sub>5</sub>	342	327
CS5	Nonamethylcyclopentasiloxane	C <sub>9</sub> H <sub>28</sub> O <sub>5</sub> Si <sub>5</sub>	356	341
CS6	Decamethylcyclopentasiloxane	C <sub>10</sub> H <sub>30</sub> O <sub>5</sub> Si <sub>5</sub>	370	355
CS7	Dodecamethylcyclohexasiloxane	C <sub>12</sub> H <sub>36</sub> O <sub>6</sub> Si <sub>6</sub>	444	429
CS8	Tetradecamethylcycloheptasiloxane	C <sub>14</sub> H <sub>42</sub> O <sub>7</sub> Si <sub>7</sub>	518	503
CS9	Decamethylcyclohexasiloxane	C <sub>10</sub> H <sub>32</sub> O <sub>6</sub> Si <sub>6</sub>	416	401
CS10	Dodecamethylcycloheptasiloxane	C <sub>12</sub> H <sub>38</sub> O <sub>7</sub> Si <sub>7</sub>	490	475
CS11	Hexamethyldioxatrisilacyclohexane	C <sub>7</sub> H <sub>20</sub> O <sub>2</sub> Si <sub>3</sub>	220	205
BS	Bicyclic siloxanes			
BS1	BS2 without two methyl groups	C <sub>8</sub> H <sub>26</sub> O <sub>7</sub> Si <sub>6</sub>	402	387
BS2	see Scheme 3	C <sub>10</sub> H <sub>30</sub> O <sub>7</sub> Si <sub>6</sub>	430	415
BS3	see Scheme 3	C <sub>12</sub> H <sub>36</sub> O <sub>8</sub> Si <sub>7</sub>	504	489
BS4	BS4 without one methyl group	C <sub>13</sub> H <sub>40</sub> O <sub>9</sub> Si <sub>8</sub>	564	549
BS5	see Scheme 3	C <sub>14</sub> H <sub>42</sub> O <sub>9</sub> Si <sub>8</sub>	578	563
TS	Tricyclic siloxanes			
TS1	see Scheme 3	C <sub>14</sub> H <sub>42</sub> O <sub>11</sub> Si <sub>9</sub>	638	623
TS2	TS1 with inserted CH <sub>2</sub> group	C <sub>15</sub> H <sub>44</sub> O <sub>11</sub> Si <sub>9</sub>	652	637
TS3	TS1 with inserted CH <sub>2</sub> and SiO <sub>2</sub> group	C <sub>15</sub> H <sub>44</sub> O <sub>13</sub> Si <sub>10</sub>	712	697
S	Silsesquioxanes (POSS)			
S1	Pentamethylsiloxanehexasilsesquioxane	C <sub>8</sub> H <sub>24</sub> O <sub>10</sub> Si <sub>7</sub>	476	461
S2	Octamethyloctasilsesquioxane	C <sub>8</sub> H <sub>24</sub> O <sub>12</sub> Si <sub>8</sub>	536	521
S3	Tetramethyldisiloxanehexasilsesquioxane	C <sub>10</sub> H <sub>30</sub> O <sub>11</sub> Si <sub>8</sub>	550	535

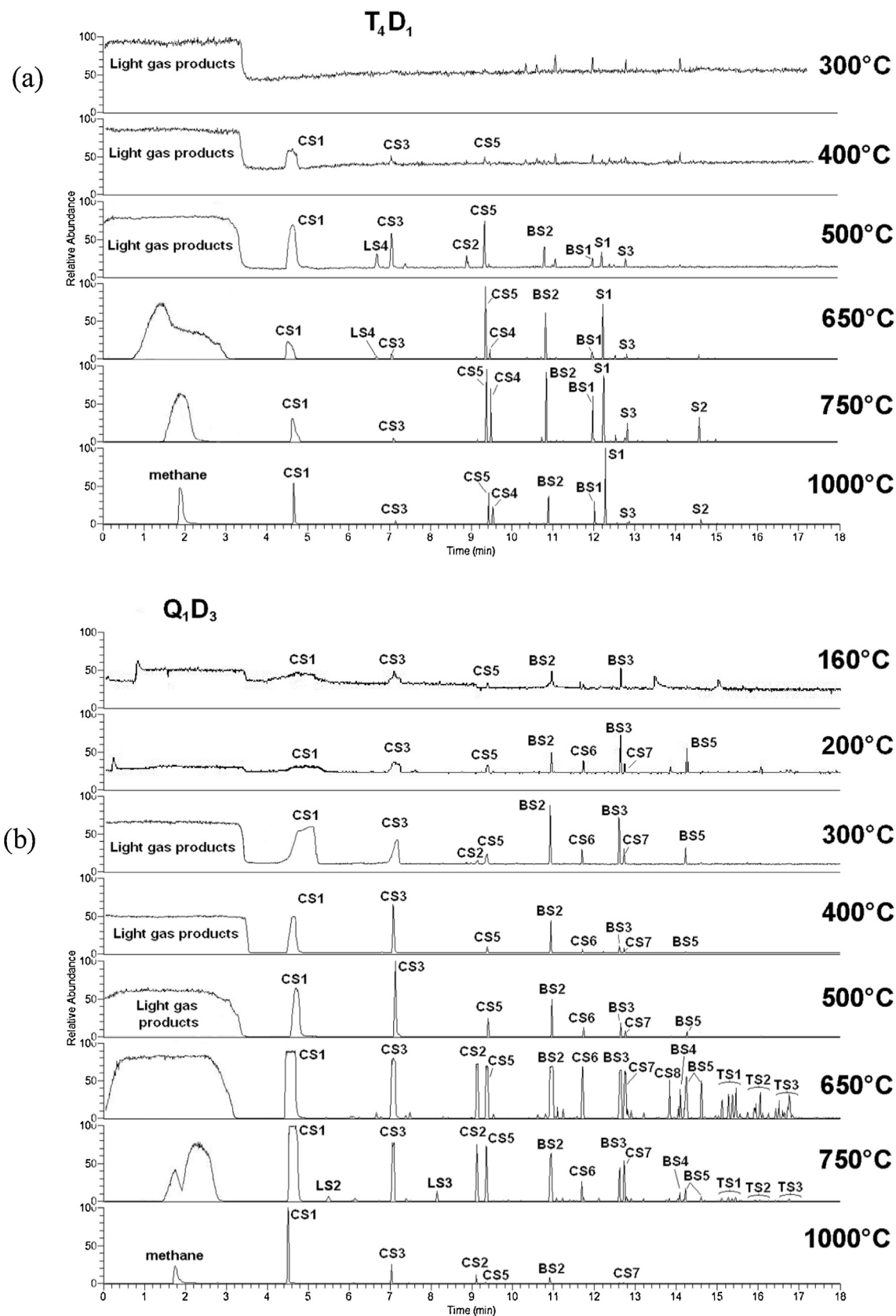
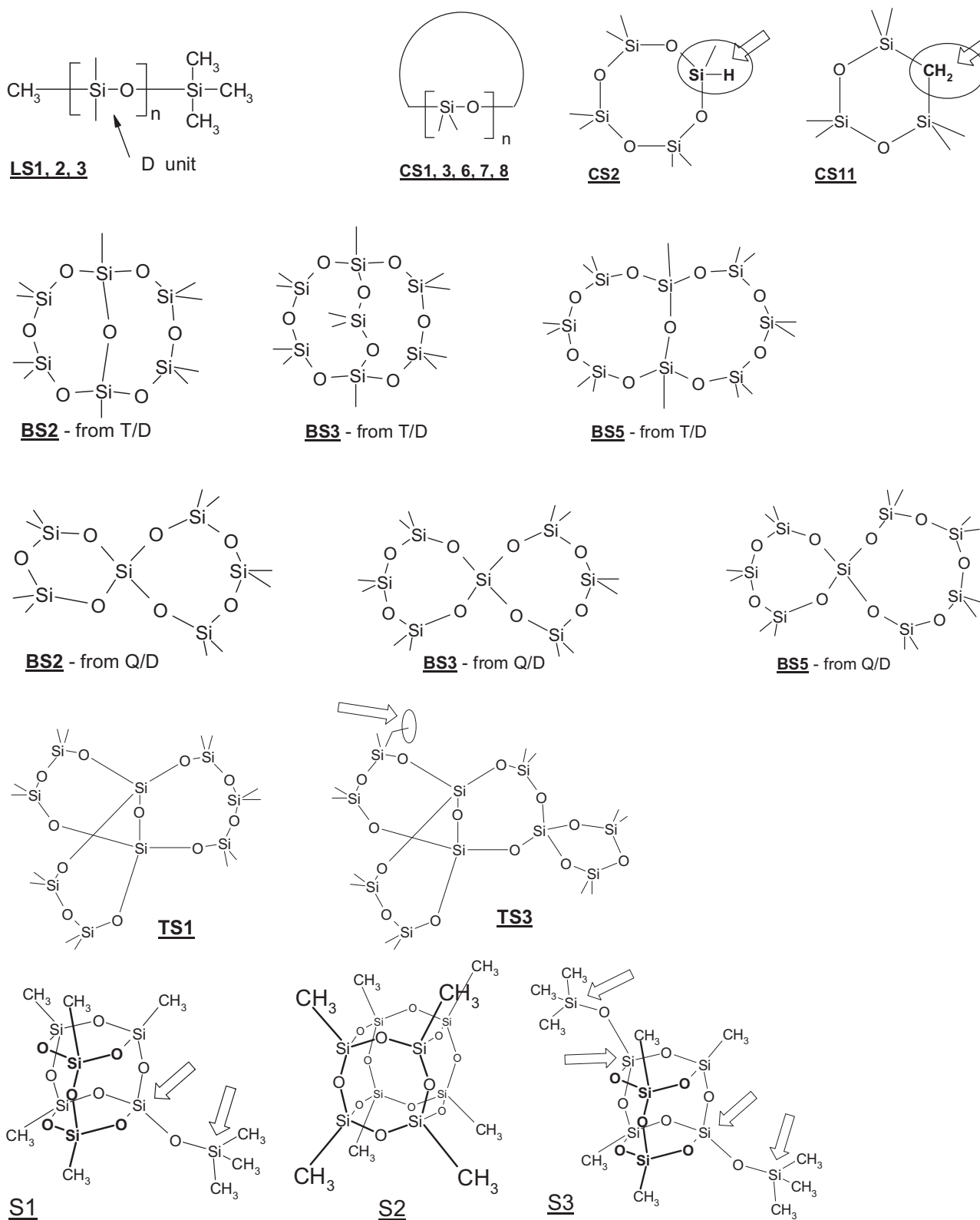


**Fig. 7.** Pyrograms of polar products from evolving from (a) the T4D1 and (b) from the Q1D3 resin, at the temperature of 160, 200 (only Q1D3), 300, 400, 500, 650, 750 and 1000°C: analysis via GC/MS using the TR-5MS chromatography column.



**Scheme 3.** The structures of the most important siloxane oligomers detected by GC/MS; sites of modification reactions are encircled and/or marked by arrows.

compounds (results: Fig. 7); and (2) the Restec Rt-Alumina column, which is highly selective for C<sub>1</sub>–C<sub>5</sub> hydrocarbons (results: Fig. 8).

### 3.2.1. Polar gases analysis

The chromatograms of the polar pyrolysis gases released from the T<sub>4</sub>D<sub>1</sub> and Q<sub>1</sub>D<sub>3</sub> precursors are shown in Fig. 7a and b, respec-

tively. These pyrolysis products belong to several types of siloxane oligomers, and are assigned in Table 2. The characteristic cations of the siloxane oligomers are formed by the loss of one methyl group. An important fragment in most of the siloxanes' MS spectra was (CH<sub>3</sub>)<sub>2</sub>SiO<sup>+</sup> (≡ D<sup>+</sup>) with m/z = 74, formed by the rupture of a Si–O bond (in some analogy to D depolymerization).

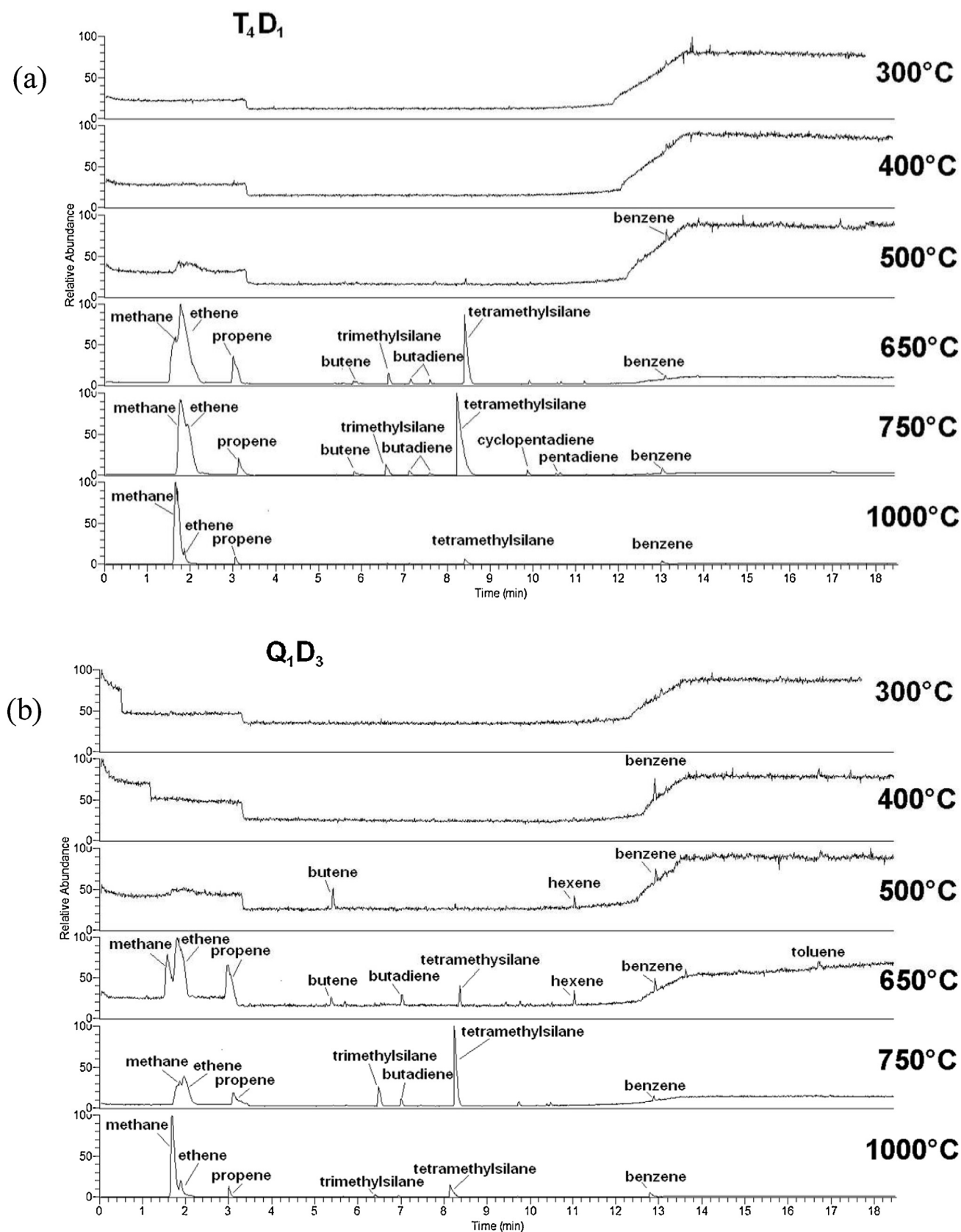


**Fig. 8.** Pyrograms of non-polar products evolving from (a) the T<sub>4</sub>D<sub>1</sub> and (b) from the Q<sub>1</sub>D<sub>3</sub> resin, analysed by GC/MS using the Restec Rt-Alumina chromatography column, recorded at pyrolysis temperatures of 300, 400, 500, 650, 750 and 1000 °C.

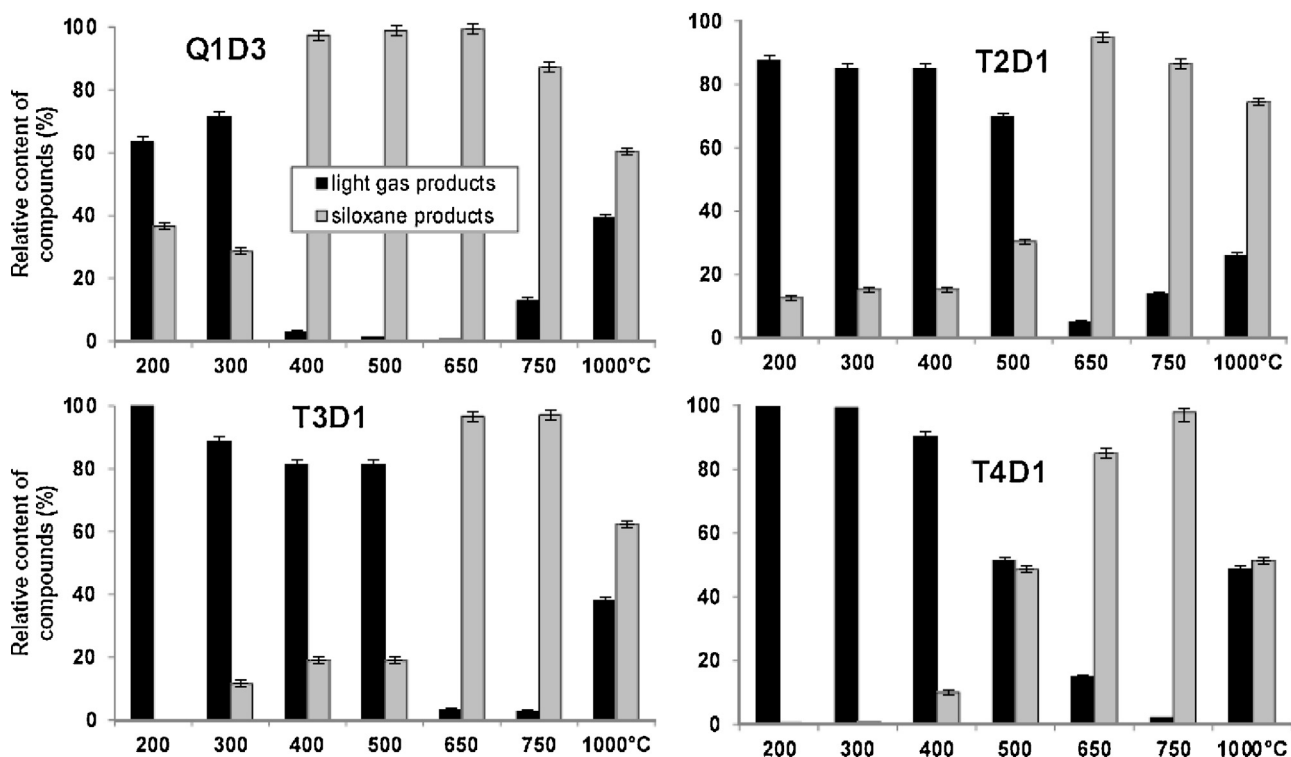


Fig. 9. Relative contents of light gaseous (hydrocarbon) products and of siloxanes in the pyrolysis gases at different temperatures, as determined for the studied precursors.

It can be seen, that at temperatures below 500 °C, where relatively small weight losses occur (Fig. 5), the (not separated) non-polar gaseous products dominate among the detected substances, or they at least represent a large fraction (in  $Q_1D_3$ ). Methane, which is an important component of the light gases fraction at 300 °C (below the temperature of Si–C bond cracking), might be formed via the side reaction  $SiOH + CH_3Si \rightarrow SiOSi + CH_4$  [21]. Additionally, remains of the toluene (used as solvent during the liquid precursor synthesis) likely contribute to the non-polar gases fraction (see also the poorly separated “mountain” at retention times above 12 min in the non-polar gases GC analysis in Fig. 8 further below).

The  $T_4D_1$  resin (see Fig. 7a, Table 2 and Scheme 3) starts to release significant siloxane amounts first at 400 °C, and richer product spectra are observed above 500 °C. This suggests a rather difficult elimination of D units. Prominent pyrolysis products are cyclic D oligomers (labelled “CS”), especially the dominant cyclo-D3 (“CS1”). Another important group are bicyclic siloxanes (labelled “BS”), which contain branching T-units as bridgeheads (see Scheme 3). At 650 and 750 °C, oligomers based purely on T units (POSS cages, labelled “S”) and their derivatives increase in prominence. It was shown by the authors in previous work [18,19], that bulkier organic groups on the T units cause an increased production of POSS oligomers. It hence can be suggested, that the mentioned

“perfect” T oligomers (POSS) are formed as by-products already during the resin cure. In addition to the perfect oligomers, some of the siloxane oligomers released by the  $T_4D_1$  resin display deviations from ideal structures based on D and T, e.g., “CS5”, “CS2”, “CS4” and “BS1”. The defects consist in methyl groups being replaced by H atoms, which indicates some Si–C bond cracking and exchange reactions on the Si atoms. Such reactions play an even greater role in the case of the POSS products released by  $T_4D_1$  at relatively high temperatures: the most prominent compound “S1” and the minor “S3” are highly modified by Si–O/Si–C exchange reactions: they contain  $SiO_4$  (Q), as well as  $Si(CH_3)_3$  (“M-type”) units, which were not present in the original T/D precursor resin. In contrast to this, the perfect T8 oligomer is only a minor POSS (“S”) product. Linear siloxanes (structure: M–D<sub>n</sub>–M; label: “LS”) also require Si–O/Si–C exchange reactions to be formed. They are found mainly among the pyrolysis products of D-rich  $T_xD_y$  resins, or of  $Q_1D_3$ . Nevertheless, the highly modified “LS4” (M-dimer with a phenyl group on one M group) is found also in case of the pyrolysis of the  $T_4D_1$  resin.

The  $Q_1D_3$  resin (see Fig. 7b and Table 2) releases siloxane oligomers already at 160–200 °C in considerable amounts, especially the low-boiling D cyclotrimer and cyclotetramer (b.p. 134 °C and 176 °C, respectively), but also cycloD5 and cycloD6 as well as the bicyclic “BS2”, “BS3” and “BS5”. The low release temperature indicates that these oligomers are already present in the cured

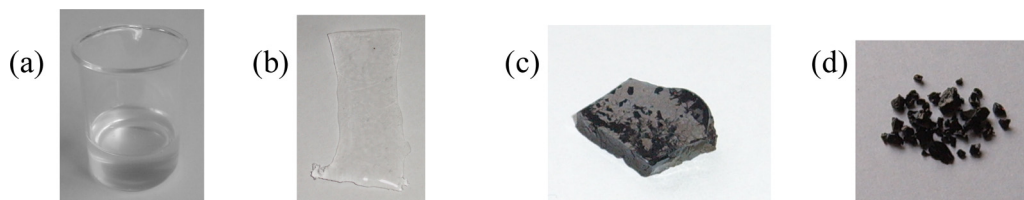
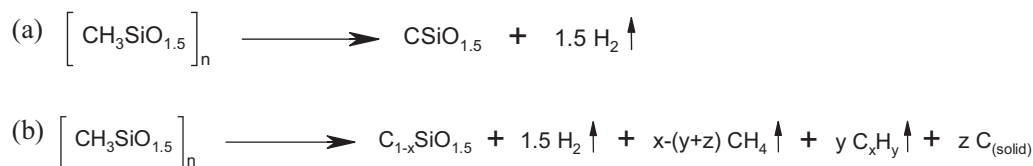


Fig. 10. Appearance of: (a) liquid oligomeric precursor solution  $T_4D_1$ , (b) of a sheet of cured polysiloxane  $T_4D_1$  (solid precursor), thickness: ca. 1.5 mm, (c) of  $SiO_2$  prepared from  $T_4D_1$  (zoomed, thickness: ca. 1.5 mm) and (d) of  $SiC$  prepared from a precursor based exclusively on the T monomer (zoomed, original platelet thickness: ca. 1.5 mm).



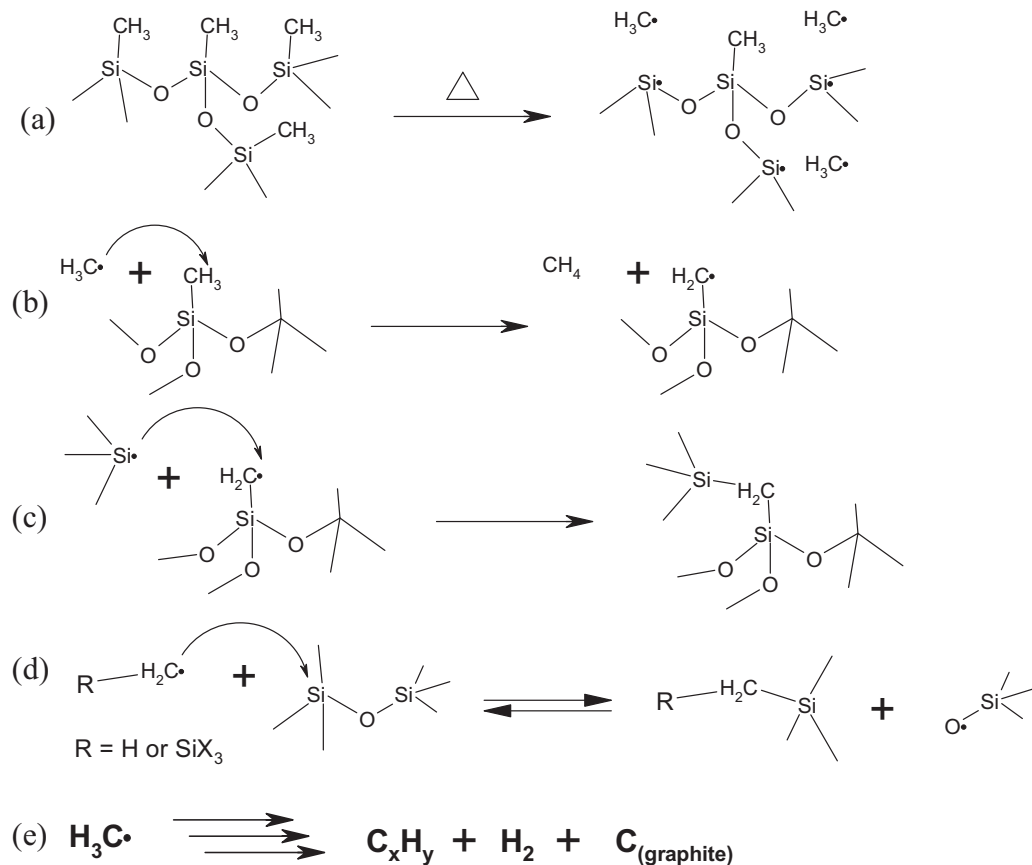
**Scheme 4.** Overall equations of the polysiloxane pyrolysis to SiOC, on the simple example of methylsilsequioxane: (a) process with no carbon loss (not observed); (b) real pyrolysis process.

precursor resin Q<sub>1</sub>D<sub>3</sub>, without any pyrolysis. The “BS” compounds released from Q<sub>1</sub>D<sub>3</sub> are spiro- isomers of their molecular-weight-analogues labelled with the same codes in Table 2, which were eliminated from T<sub>x</sub>D<sub>y</sub> resins (one Q and one D unit in the spiro-isomer replace two T units in the T/D bicyclic isomer).

As the pyrolysis temperature increases to 650 and 750 °C, the prominence of the larger monocyclic “CS” as well as of the bicyclic (spiro) “BS” products markedly increases, as result of elimination reactions. Additionally, tricyclic oligomers “TS” (with two four-functional Q bridgeheads) are also released. In this temperature range, exchange reactions already are prominent (see discussion below), thus leading to new species from the “CS”, “BS” and “TS” product families, as well as to the appearance of the simple linear siloxanes “LS2” and “LS3” (see Table 2). Noteworthy is the minor product “CS11” which is a cycloD3 molecule in which a ring-O-atom is replaced by a CH<sub>2</sub> group. At 1000 °C the spectrum of pyrolysis gases released from Q<sub>1</sub>D<sub>3</sub> is very simple, in some contrast to the T<sub>4</sub>D<sub>1</sub> precursor: only methane and cycloD3 are prominent, accompanied by small amounts of cycloD4.

### 3.2.2. Non-polar pyrolysis gases

Fig. 8a and b shows the GC analyses of non-polar products evolving from the T<sub>4</sub>D<sub>1</sub> and Q<sub>1</sub>D<sub>3</sub> precursors, respectively. The volatile non-polar compounds were previously detected on the TR-5MS column only as one broad large peak at the retention time 1–4 min. Hydrocarbons formed by the thermolysis of methyl groups, such like alkanes (methane), alkenes (ethene, propene, butene, hexene), alkadienes (butadiene, pentadiene), cycloalkadienes (cyclopentadiene) and aromates (benzene, toluene) were detected among the pyrolysis gases. A part of the higher hydrocarbons, which does not manage to escape from the sample, becomes the source (via further thermolysis) of the C-rich (“graphite”) domains in the pyrolytic SiOC. The non-polar silicon compounds trimethylsilane and tetramethylsilane, which are formed via Si–O/Si–C exchange reactions, were also detected as prominent non-polar pyrolysis products. Generally, the product spectra of the non-polar pyrolysis gases were very similar in case of the Q<sub>1</sub>D<sub>3</sub> and T<sub>4</sub>D<sub>1</sub> precursors. At 1000 °C, the spectrum of non-polar products becomes simple for all precursors: methane is the only major component. Both the



**Scheme 5.** (a) First pyrolysis step: Si–C bond cracking; Important exchange reactions during pyrolysis: (b) hydrogen exchange between methyl radicals and e.g., methyl groups; (c) methylene bridge formation from the product of the reaction “b” and a silyl radical; (d) exchange reactions, in which Si–C bonds are exchanged for Si–O bonds and vice versa, which lead to the formation of SiO<sub>2</sub>– and SiC-rich nanodomains; (e) hydrogen exchange reactions between methyl radicals, which lead to the escape of hydrocarbons and of hydrogen, as well as to the formation of “graphite” nano-domains.

analysis of polar and non-polar pyrolysis products (Figs. 7b and 8b, respectively) indicates that efficient Si–O/Si–C exchange reactions occur during the pyrolysis of the Q<sub>1</sub>D<sub>3</sub> resin between escaping D units and branching (skeleton-) Q units. Without these reactions, the Q<sub>1</sub>D<sub>3</sub> precursor would lose all D units and yield pure SiO<sub>2</sub>, which is not observed (see above-discussed EDX analysis).

The approximate ratio of the released non-polar hydrocarbon gases to the siloxane compounds was estimated from the chromatograms with the TR-5MS column, like the ones in Fig. 7, where the non-polar gases appear as one broad “mountain”. The result is shown in Fig. 9. The columns in Fig. 9 symbolize only the relative amounts (their sum is 100% for a given temperature) of light gases and siloxanes. The total amounts of released volatiles, which greatly depend on resin type and on temperature, are not given by Fig. 9 (but could be estimated from the weight losses in Figs. 3 and 4). The influence of the amount of D in the precursor can be clearly seen: D-rich precursor resins, especially Q<sub>1</sub>D<sub>3</sub>, release siloxane-rich gases already at relatively low temperatures (400 °C: oligomers evaporation, and some easy elimination reactions). The T<sub>x</sub>D<sub>y</sub> resins generally start to release siloxane-rich gases at higher temperatures, at 650 °C and above, as consequence of elimination reactions. The relative content of non-polar gases reaches a minimum between 650 and 750 °C; thereafter it increases again, as consequence of methyl group thermolysis and of Si–O/Si–C exchange reactions.

### 3.3. Compactness, cracking and “micro-creep” during pyrolysis

Colorless, clear solutions of liquid precursor resins Q<sub>1</sub>D<sub>3</sub>, T<sub>2</sub>D<sub>1</sub>, T<sub>3</sub>D<sub>1</sub>, and T<sub>4</sub>D<sub>1</sub> (Fig. 10a) were cured to compact colorless and transparent solid precursors (Figs. 10b and 11a). After the pyrolysis up to 1000 °C, shiny black SiOC samples were obtained, which were typically compact (Fig. 10c). If a methylsiloxane precursor based entirely on the T monomer was used as SiOC precursor, however, the sample displayed an excessive tendency to cracking (see Fig. 10d), if pyrolyzed under the same conditions like Q<sub>1</sub>D<sub>3</sub>, T<sub>2</sub>D<sub>1</sub>, T<sub>3</sub>D<sub>1</sub>, and T<sub>4</sub>D<sub>1</sub>.

The co-monomer D hence seems to reduce the tendency to cracking of SiOC samples prepared from polysiloxanes: already during the authors' previous studies [18,19] it was observed, that pyrolytic SiOC specimens obtained from D-rich precursor compositions typically displayed very smooth shapes and surfaces. SEM micrograms of break surfaces of the prepared SiOC samples demonstrate, that at the lowest D contents in the precursor, the pyrolysed samples display an increased tendency to micro-cracks (see Figs. 11c and 10d). At the highest D contents in the precursor (T<sub>2</sub>D<sub>1</sub>, Q<sub>1</sub>D<sub>3</sub>), the pyrolyzed samples displayed pores sized tens of micrometers (Fig. 11b), in spite of the precursor being highly compact prior to pyrolysis (Fig. 11a). The formation of such large pores, as well as the excessive cracking of the resin based entirely on T seem to suggest, that the chemistry of the D co-monomer makes possible some temporary micro-creep (plastic deformation) during the course of the pyrolysis (see discussion further below).

### 3.4. Post-pyrolysis of completely pyrolyzed (1000 °C) SiOC samples

In order to assess the completion of the pyrolysis conversion polysiloxane → SiOC in the samples heated up to 1000 °C in nitrogen, pyrolysis-GC/MS analysis of the final SiOC products obtained from the Q<sub>1</sub>D<sub>3</sub>, T<sub>2</sub>D<sub>1</sub>, T<sub>3</sub>D<sub>1</sub>, and T<sub>4</sub>D<sub>1</sub> precursors was carried out. In the ideal case it would be expected, that after pyrolysis up to 1000 °C, the samples would display no more weight losses, and that only trace amounts of pyrolysis gases would escape, which would display the rather simple compositions observed in Fig. 7 for 1000 °C.

Eventual further weight losses resulting from post-pyrolysis heating – at the constant temperature of 1000 °C for 4 h in nitrogen – were assessed by weighing selected SiOC samples before and after such a treatment. The weight losses were expectedly found to be negligible, not higher than 0.3%, which was below the experiments' accuracy.

On the other hand, contrarily to expectation, the pyrolysis-GC/MS analyses indicated, that the traces of pyrolysis gases released from the SiOC samples after pyrolysis up to 1000 °C still are component-rich, especially if the samples were heated to temperatures not exceeding 750 °C. In fact, the product spectra released at different temperatures from SiOC samples produced from Q<sub>1</sub>D<sub>3</sub> and T<sub>4</sub>D<sub>1</sub> (see Supporting information, SI-Fig. 1) are nearly identical with the spectra released at the same temperatures during the pyrolysis of the respective precursors (see Fig. 7). The only noteworthy difference is the somewhat smaller content of the non-polar gases in the “post-pyrolysis gases” at lower post-pyrolysis temperatures. The above observations indicate the presence of some pyrolyzable siloxane and hydrocarbon depositions in micro- or nano-pores of the SiOC products.

## 4. Discussion

### 4.1. Chemistry of the siloxane pyrolysis to SiOC

The siloxane pyrolysis is seemingly a simple process, which in the ideal case would be represented by Scheme 4a, where the polysiloxane polymer would transform to SiOC by only losing the hydrogen from the methyl groups. In reality, the pyrolysis chemistry is more complex (Scheme 4b): besides H<sub>2</sub>, also hydrocarbons are formed as gaseous products. A part of them escapes, while another part participates in exchange reactions (e.g., as methyl radicals), or is thermolyzed to carbon and hydrogen. The hydrocarbons' thermolysis yields C-rich and eventually graphitic domains in the pyrolytic SiOC [2,22], which are responsible for the black color of the final product.

The key reactions of polymethylsiloxane pyrolysis to SiOC have been described in the literature [16,17]. At the beginning of the pyrolysis, some Si–OH + Si–OH condensation (final stages of the cure reaction shown as the step 2 of the Scheme 2) can occur to a small extent, generating water vapor. Also the condensation side reaction: SiOH + CH<sub>3</sub>Si → SiOSi + CH<sub>4</sub> can occur and generate some methane at relatively low temperatures [21]. True pyrolysis reactions begin at temperatures around 400 °C, starting with the cracking of Si–C bonds (see Scheme 5a) which are less stable than C–H bonds (dissociation energies are 318 and 413 kJ/mol, respectively). In the case of the polysiloxane composed exclusively of the T monomer, the three-dimensional Si–O skeleton of the polymer is thermally very stable and should resist pyrolysis temperatures well above 1000 °C (similarity with the SiO<sub>2</sub> network). On the other hand, the Si–O skeleton can be attacked by free or Si-bonded methyl radicals (Scheme 5d) and subsequently undergo Si–O/Si–C exchange reactions [16,17], which can modify it by disconnecting bonds and by forming new ones. As result of the exchange reactions, a distribution of SiC<sub>4</sub>, SiOC<sub>3</sub>, SiO<sub>2</sub>C<sub>2</sub>, SiO<sub>3</sub>C and SiO<sub>4</sub> units replaces the original SiO<sub>3</sub>C (“T”) units. The methyl radicals, which were split from the Si–O skeleton, can react with methyl groups still bonded to Si, which in turn can undergo exchange or radical recombination reactions, thus yielding Si–C–Si bridges (Schemes 5b and 6c) [16]. These bridges are the starting structures for the formation of molecular SiC segments in silicon oxycarbide. The methyl radicals also can react with each other under formation of hydrocarbons, and eventually of C-rich (“graphite”) domains and of hydrogen (Scheme 5e). Reduction of the Si–O skeleton with graphite or with the escaping hydrogen never occurs below 1700 °C [23], hence no Si–Si bonds

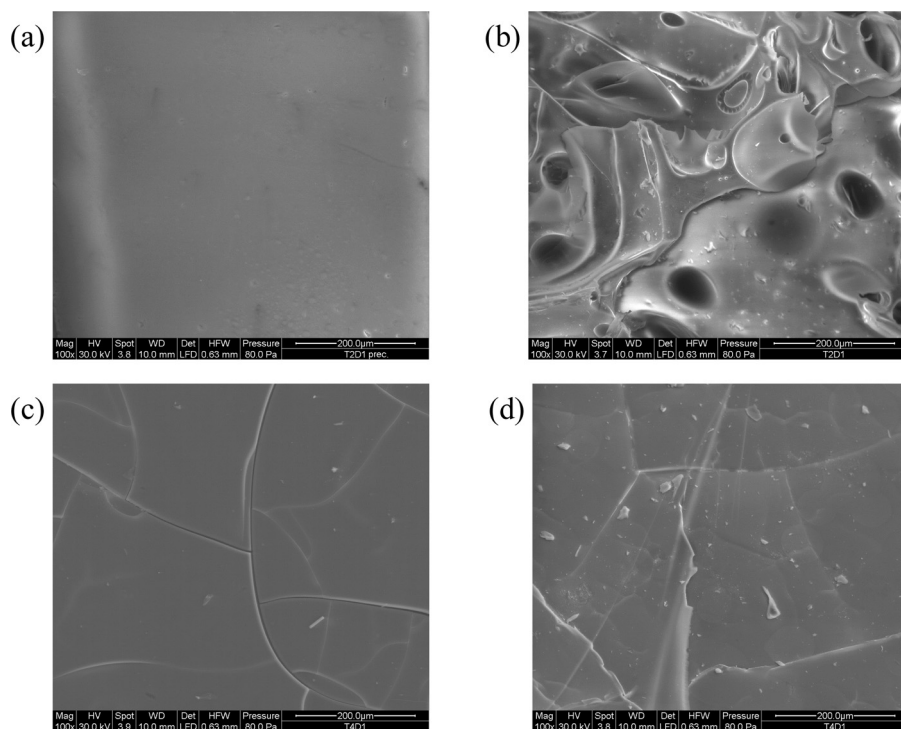


**Fig. 11.** Micro-scale morphology of (a) T2D1 cured siloxane precursor, (b) of the same T2D1 after pyrolysis to SiOC and (c), (d) of pyrolysed T4D1.

are formed. Pores, eventually very small ones, are formed during the pyrolysis as result of the escape of a part of the methyl groups, and were described in literature [10,11], including nanometer-sized pores in seemingly compact SiOC [6].

#### 4.2. Chemical effects of the incorporation of the co-monomer D

If the linear co-monomer D is incorporated alongside the branching T in the precursor resin, the above discussed basic pyrolysis reactions remain unchanged, but some additional effects appear:

During the sol-gel synthesis (Scheme 2) of the polysiloxane precursor resin, cyclic low-molecular-weight D oligomers are formed as volatile by-products (cyclo-D3: b.p. = 134 °C, cyclo-D4: b.p. = 176 °C), as well as bicyclic and tricyclic mixed oligomers with incorporated T or Q units. Also the branching oligomer T can form small spherical oligomers, as was observed by pyrolysis-GC/MS (Fig. 7a, product “S2”), but this occurs only to a small extent, for steric and statistical reasons.

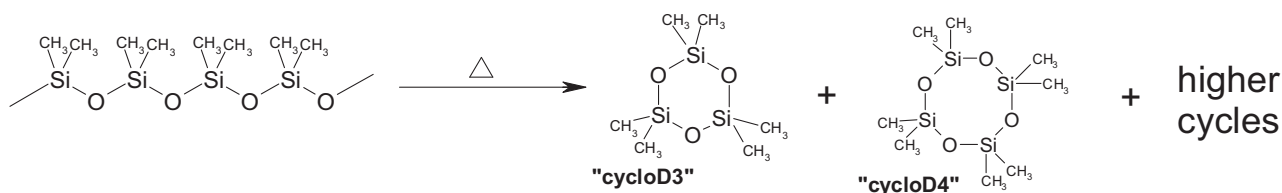
Another important effect is, that the D units incorporated in the three-dimensional polymer network can eliminate, thus causing rearrangements of the Si–O skeleton. The thermal depolymerisation of simple polydimethylsiloxane (poly-D), which starts even below 300 °C (Scheme 6), is known in the literature [24–26]. The D units eliminated from the studied resins can escape from the samples as gaseous cycloD- or as D/T or D/Q oligomers, but they also can take part in the Si–O/Si–C exchange reactions, as was markedly observed on the example of the  $Q_1D_3$  system. The eliminated D units hence can be expected to participate in exchange reactions also during  $T_xD_y$  pyrolysis (e.g., in the formation of modified POSS species “S1” and “S3”). The exchange reactions with the escaping and highly mobile D oligomers hence can contribute to the reorganization of the precursor’s Si–O skeleton, and thus they may play a role in the below-discussed temporary micro-creep of these pyrolyzing materials.

The weight losses caused by evaporation of cycloD-, D/T and D/Q oligomers, which were present as by-products in the precursor resins, may overlap in temperature with thermally induced eliminations of oligomers from the resins’ polymer network. The larger oligomers namely possess relatively high boiling points, while some eliminations, e.g., of D from D-sequences (Scheme 6) might occur already at relatively low temperatures (300 °C). On the other hand, the more difficult eliminations of single D units from the polymer network (Scheme 8) require higher temperatures, above 500 °C, at which already the Si–C bond cracking and the Si–O/Si–C exchange reactions become prominent. As result of the overlap of the temperature ranges of the elimination and of the exchange reactions, some siloxane oligomers released at high pyrolysis temperatures undergo modifying reactions like demethylation, methylation, or Si–O/Si–C exchange (e.g., T groups modified to Q or M). Marked examples are the hexameric POSS derivatives labelled “S1” and “S3” in Fig. 7a (see also Scheme 3), released from  $T_4D_1$ : not only their modification, but also their disconnection from the pyrolysing polymer network might be caused by the exchange reactions.

In case of D-rich resins like  $Q_1D_3$ , where both the evaporation and the elimination of D, D/T and D/Q oligomers are prominent, the temperature ranges of the mentioned processes can be recognized by evaluation of the pyrolysis-GC/MS spectra (Fig. 7b): at first, the GC-peaks of siloxane oligomers display high intensities in the temperature range of 160–300 °C, indicating evaporation of already existing oligomers. Thereafter, at 400 and 500 °C the intensity of the oligomers’ peaks markedly decreases. At 650 °C, the intensity of the oligomers’ peaks dramatically increases again and the product spectrum becomes richer, indicating oligomers formation via elimination reactions.

#### 4.3. Possibility of plastic deformation during pyrolysis

A very interesting and important aspect of the polysiloxanes’ pyrolysis is the possibility vs. impossibility of temporary micro-



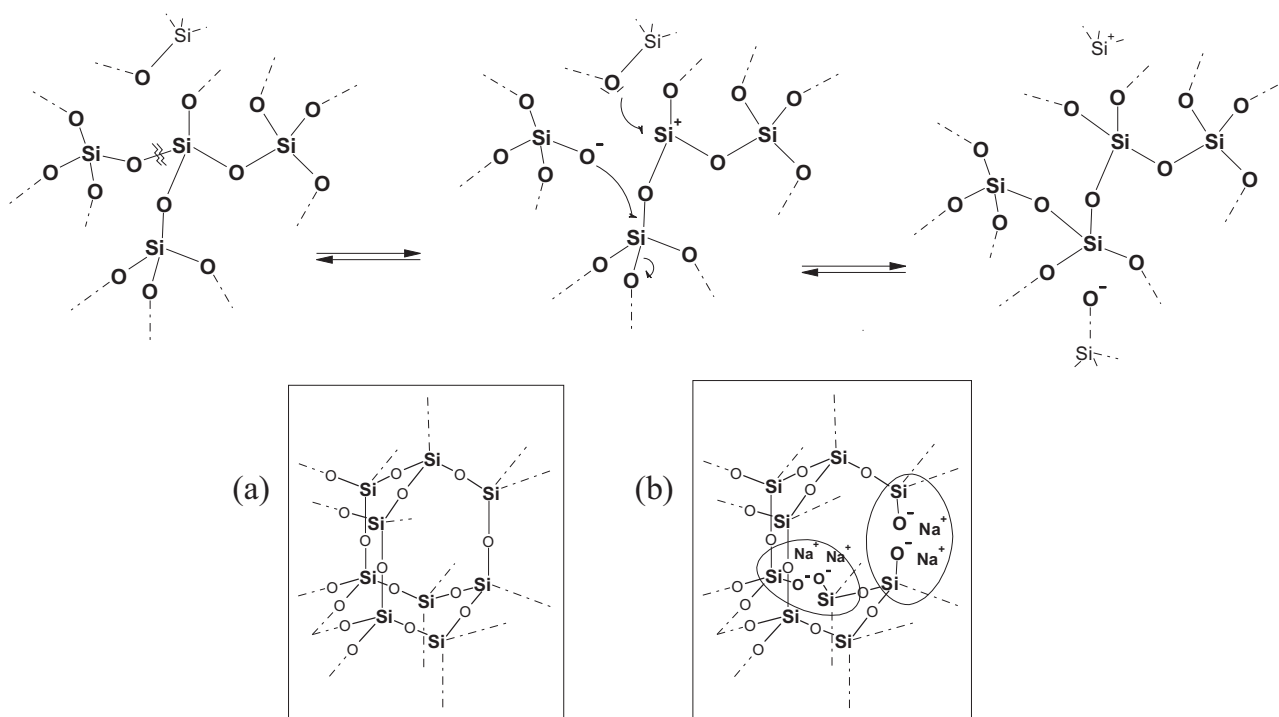
**Scheme 6.** Thermal depolymerization of polydimethylsiloxane.

scopic plastic deformations (flow, creep) during this process: a complete impossibility of plastic deformations would mean, that stresses building up as result of the local formation of a more compact inorganic structure would occasionally cause irreparable cracks in large bulk material pieces, thus strongly reducing their toughness. On the other hand, the temporary possibility of microscopic plastic deformations would lead to stress relaxation, to some crack healing, and – in case of excessive gas release – also to the formation of a microscopic pore system, which would make possible a smooth gas escape.

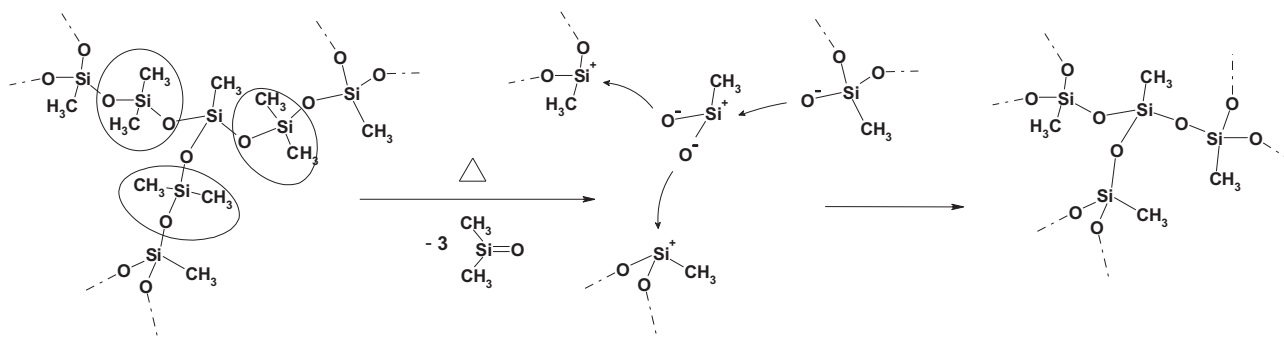
The simplest representative of the studied siloxane resins is poly(methylsilsesquioxane), which consists entirely of the branching T monomer. Structurally, this polymer is chemically related both to polydimethylsiloxane (PDMS) and to silicon dioxide ( $\text{SiO}_2$ ). The latter is a covalent 3-D network, which melts at  $1703^\circ\text{C}$  [23], via the ionic dissociation of  $\text{Si-O}$  bonds to  $(-\text{O})_3\text{Si}^+$  cations and  $(-\text{O})_3\text{Si-O}^-$  anions, followed by electrophilic (on O) and nucleophilic (on Si) substitutions performed by these ions on neighboring structure segments, as illustrated in Scheme 7. In the case of amorphous  $\text{SiO}_2$ , the glass transition temperature, above which plastic deformations (bond reorganization, like melt flow) are possible, is in the range of  $1300^\circ\text{C}$ . As result of the ionic dissociation, the conductivity of the  $\text{SiO}_2$  melt increases with rising temperature [23]. The energy-consuming splitting of the strong covalent  $\text{Si-O}$  bonds to ion pairs is the reason for the high melting point (and for the high glass transition temperature) of  $\text{SiO}_2$ . On the other hand, in

silicate glasses (see Scheme 7, inlay (b)), the  $(-\text{O})_3\text{Si-O}^-$  anions are already present at room temperature, as result of alkaline oxides incorporation. The presence of the anions shifts down the temperature of glass transition ( $T_g$ ) by some  $700^\circ\text{C}$  in comparison to quartz glass, to  $T_g$  values around  $600^\circ\text{C}$ . The highly crosslinked polysiloxane based entirely on T units possesses neither anions (like silicate glasses) nor a high segmental mobility of the repeat units like the easily depolymerizing PDMS. Hence the hypothetical melting point of the  $\text{Si-O}$  skeleton of poly(T) likely will be close to the  $T_g$  of quartz glass ( $1300^\circ\text{C}$ ).

In contrast to  $\text{SiO}_2$  and to the T-resin, temporary micro-flow should be possible in the  $\text{T}_x\text{D}_y$  copolymers (see mechanism suggested in Scheme 8), from which a large part of the D co-monomer eliminates relatively easily (due to higher segmental mobility of D units), as the above discussed experiments demonstrated. The elimination of D (or of oligomeric D/T segments) leaves disconnected T units, which eventually irreversibly bond together. A temporary material micro-flow is hence achieved. According to the above TGA and pyrolysis gases analyses, the temperature range of D eliminations overlaps with the range of the  $\text{Si-C}(\text{H}_3)$  bond cracking and of the subsequent exchange reactions. Thus the temporary micro-flow coincides with the final reorganization of bonding in the pyrolysing material. Bond reorganizations caused by exchange reactions between the polymer skeleton and the highly mobile escaping D units also might further contribute to the temporary micro-flow. Smooth surfaces and compact shapes of pyrolysed D-



**Scheme 7.** Mechanism of melting and flow of  $\text{SiO}_2$  (3-D network); inlay (a): structure of cristoballite- $\text{SiO}_2$ ; inlay (b): structure of a glass with an  $\text{O}^{2-}:\text{SiO}_2$  ratio of 1: 4.5 (typical value in commercial glasses is between 1:3 and 1:4).

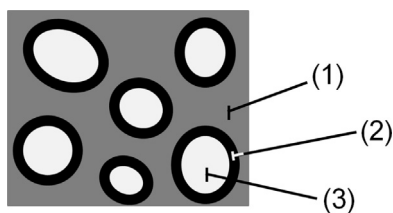


**Scheme 8.** Elimination of D units from a T/D siloxane resin: bond disconnection followed by formation of new bonds, which temporarily makes possible some segmental movement, and hence shape change or crack healing.

rich  $T_xD_y$  samples, which displayed considerable weight losses on one hand, and the cracking of the resin based entirely on the T monomer on the other, can be well explained by the above suggested micro-flow mechanism. Another argument for the occurrence micro-flow in  $T_xD_y$  resins are the smooth macroscopic pores formed after the pyrolysis of  $T_xD_y$  resins with high D contents (e.g.,  $T_1D_2$ ), which were observed by the authors in their previous work [19]. Due to the generally very similar pyrolysis chemistry, analogous micro-flow effects like in  $T_xD_y$  are expected also in pyrolysing Q/D resins. A schematic overview of the temperature ranges of the processes during polysiloxane pyrolysis is given in SI-Fig. 2.

#### 4.4. Pyrolysis of sediments in the pores of the fully pyrolyzed SiOC

A very interesting result found in this work is the ability of the prepared SiOC samples to release further gases even after having undergone pyrolysis up to 1000 °C. The transformation to inorganic glass was found to be quantitative after such a treatment, as reported in previous work [27] by the authors. The likely source of the pyrolysis gases are micrometer- and nanometer-sized pores in the prepared SiOC. The existence of such pores is suggested by the relatively low density of pyrolytic SiOC around 2.0 g/cm<sup>3</sup> as determined e.g., by the authors in [19]; compared with quartz: 2.65 and SiC: 3.21 g/cm<sup>3</sup> [23], although typical samples of pyrolytic SiOC appear smooth even under microscope. The occurrence of nano-porosity in SiOC has been already directly proven in the literature [6]. Hence, pyrolysis gases, which did not escape from the samples during pyrolysis, most likely condense or polymerize to easily degradable compounds on pore walls upon sample cooling, as suggested in Scheme 9. In case of foamy samples with macroscopic pores, such depositions were directly observed by the authors in their previous work [19], by means of EDX elemental analysis, as carbon-rich regions on the surface of pores. The hydrocarbons generated by the previous pyrolysis, as well as cycloD, D/T and D/Q oligomers, are all C-rich in comparison with the original polysiloxane, or with SiOC. These sediments obviously release pyrolysis gases very similar to the original ones upon renewed heat-



**Scheme 9.** Macro-pores (3) in the SiOC matrix (1) as found in previous work, whose walls are covered by carbon-rich material (2); this sediment deposited from pyrolysis gases is the likely source of volatile compounds detected upon repeated heating of pyrolyzed samples.

ing, via evaporation or deolymization. At higher temperatures, re-forming of the released gases likely takes place, in full analogy to the mutual interactions of pyrolysis gases during the “original” pyrolysis.

## 5. Conclusions

- It was demonstrated, that the presence of the D units can be correlated with the useful temporary “micro-creep” ability of the pyrolyzing material, thus reducing its tendency to cracking, and even making possible the formation of macroscopic pores in the previously compact precursor.
- The co-monomer D is responsible for increased weight losses during polysiloxane pyrolysis to SiOC, if it is present in larger amounts. It escapes via thermal elimination in the form of cyclic D-oligomers, but also in the form of bicyclic and tricyclic oligomers, in which the branching main monomer is incorporated. Some of the oligomers are already formed during the sol-gel synthesis of the polymeric precursor resin. There is an approximately linear correlation between the D-units content and the observed pyrolysis weight loss (which corresponds to ca. 50% of D units).
- The weight loss investigations also show that a significant part of the D units (ca. 50%) is incorporated into the SiOC glass, after undergoing Si–O/Si–C exchange reactions. This is especially marked in the case of the Q1D3 resin, which does not contain carbon in the branching Q(silicate) units, and which contains a large excess of D units (if compared to the investigated T/D resins): a large part of the D units is incorporated in the pyrolysate, thus yielding a standard SiOC product, and numerous intermediates of the exchange reactions are clearly detectable by GC/MS.
- An interesting finding was that after completed pyrolysis at 1000 °C, the obtained SiOC products still can release pyrolysis gases detectable by GC/MS upon repeated heating, even if no significant weight losses are observed: this indicates the presence of small amounts of pyrolysable sediments in micro- and nano-pores of the SiOC glass.

## Acknowledgements

This work was carried out thanks to the Operational Program Prague—Competitiveness, project “Centre for Texture Analysis” (No.: CZ.2.16/3.1.00/21538), and to the long-term conceptual development of research organisation RVO: 67985891.

## Appendix A. Supplementary data

Supplementary data associated with this article can be found, in the online version, at <http://dx.doi.org/10.1016/j.jaap.2015.12.018>.

## References

- [1] C.G. Pantano, A.K. Singh, H. Zhang, *J. Sol–Gel Sci. Technol.* 14 (1999) 7–25.
- [2] H.J. Kleebe, Y.D. Blum, *J. Eur. Ceram. Soc.* 28 (2008) 1037–1042.
- [3] P. Du, X.N. Wang, I.K. Lin, X. Zhang, *Sens. Actuators A Phys.* 176 (2012) 90–98.
- [4] H. Brequel, J. Parmentier, G.D. Sorarù, L. Schiffini, S. Enzo, *Nanostruct. Mater.* 11 (1999) 721–731.
- [5] M. Černý, P. Glogar, Z. Sucharda, Z. Chlup, J. Kotek, *Composites* 40 (2009) 1650–1659.
- [6] L.Q. Duan, Q.S. Ma, *Ceram. Int.* 38 (2012) 2667–2671.
- [7] J. Wu, Y. Li, L. Chen, Z. Zhang, D. Wang, C. Xu, *J. Mater. Chem.* 22 (2012) 6542–6545.
- [8] M. Weinberger, S. Puchegger, T. Froeschl, F. Babonneau, H. Peterlik, N. Husing, *Chem. Mater.* 22 (2010) 1509–1520.
- [9] C. Vakifahmetoglu, P. Colombo, A. Pauletti, C. Fernandez Martin, F. Babonneau, *Int. J. Appl. Ceram. Technol.* 7 (2010) 528–535.
- [10] J. Cordelair, P. Greil, *J. Eur. Ceram. Soc.* 20 (2000) 1947–1957.
- [11] T.E. Twardowski, T. Twardowski, *Introduction to Nanocomposite Materials: Properties, Processing, Characterization*, DEStech Publications Inc., Lancaster, Pennsylvania, USA, 2007, ISBN: 978-1-932078-54-1.
- [12] L.F. Chen, Z.H. Cai, W. Zhou, L. Lan, X.J. Chen, *J. Mater. Sci.* 40 (2005) 3497–3501.
- [13] M. Černý, A. Strachota, Z. Chlup, Z. Sucharda, M. Žaloudková, P. Glogar, *J. Compos. Mater.* 47 (2013) 1055–1066.
- [14] M. Černý, P. Glogar, Z. Sucharda, *J. Compos. Mater.* 43 (2009) 1109–1120.
- [15] M. Černý, Z. Sucharda, A. Strachota, Z. Chlup, P. Glogar, *Ceram. Silik.* 54 (2010) 295–403.
- [16] R. Camprostrini, G. D'Andrea, G. Carturan, R. Ceccato, G.D. Sorarù, *J. Mater. Chem.* 6 (1996) 585–594.
- [17] H.P. Mutin, *J. Am. Ceram. Soc.* 85 (2002) 1185–1189.
- [18] A. Strachota, M. Černý, P. Glogar, Z. Sucharda, M. Havelcová, Z. Chlup, I. Dlouhý, V. Kozák, *Acta Phys. Pol. A* 120 (2011) 326–330.
- [19] A. Strachota, M. Černý, Z. Chlup, M. Šlouf, J. Hromádková, J. Pleštil, H. Šandová, P. Glogar, Z. Sucharda, M. Havelcová, J. Schweigstillová, I. Dlouhý, V. Kozák, *J. Non-Cryst. Solids* 358 (2012) 2771–2782.
- [20] J.C. Kleinert, C.J. Weschler, *Anal. Chem.* 52 (1980) 1245–1248.
- [21] M. Blazso, G. Garzo, T. Szekeley, *Chromatographia* 5 (1972) 485–492.
- [22] F. Kolar, V. Machovic, J. Svitilova, L. Borecka, *Mater. Chem. Phys.* 86 (2004) 88–98.
- [23] A.F. Holleman, E. Wiberg, N. Wiberg, *Inorganic Chemistry*, Academic Press, Waltham, Massachusetts, USA, 2001, ISBN-13: 978-0123526519; SiO<sub>2</sub>: pages 854–859; silicate glasses: pages 883–890; silanes and alkylsilanes: pages 844–846.
- [24] J.P. Lewicki, J.J. Liggit, M. Patel, *Polym. Degrad. Stab.* 94 (2009) 1548–1557.
- [25] M.G. Voronkov, *J. Organomet. Chem.* 557 (1998) 143–155.
- [26] J.C. Kleinert, C.J. Weschler, *Anal. Chem.* 52 (1980) 1245–1248.
- [27] J. Brus, F. Kolar, V. Machovic, J. Svitilova, *J. Non-Cryst. Solids* 289 (2001) 62–74.